Room Temperature Excitation-Emission Spectra of Single LH2 Complexes Show Remarkably Little Variation

Esther Gellings†, Richard J. Cogdell‡ and Niek F. van Hulst†§*

† ICFO − Institut de Ciències Fotòniques, The Barcelona Institute of Science and Technology, 08860 Castelldefels, Barcelona, Spain

‡ Davidson Building, Institute of Molecular, Cell and Systems Biology, College of Medical, Veterinary and Life Sciences, University of Glasgow, Glasgow G12 8QQ, UK

§ ICREA − Institució Catalana de Recerca i Estudis Avançats, 08010 Barcelona, Spain

Corresponding Author

* E-mail: Niek.vanHulst@ICFO.eu

ABSTRACT

Excitation spectroscopy gives direct insight in excited state manifold, energy transfer, transient intermediates, vibrations, etc. Unfortunately, excitation spectroscopy of single molecules at ambient conditions has remained challenging. Here, we present excitation spectra alongside emission spectra of the same individual light harvesting complex LH2 of the purple bacteria Rps. acidophila. Acquisition of both the excited and ground state spectra allows to quantify disorder and interband correlations, which are key variables for the interpretation of observed long-lasting coherences. We have overcome the low photostability and small fluorescence quantum yield, inherent to many biologically relevant systems, by combining single molecule Fourier transform spectroscopy, low excitation intensities, and effective data analysis. We find that LH2 complexes show little spectral variation (130-170 cm^{-1}), that their two absorption bands (B800-B850) act uncorrelated, and that the Stokes shift is not constant. The low amount of spectral disorder underlines the protective role of the protein scaffold, benefitting the efficient energy transport throughout the light-harvesting membrane.

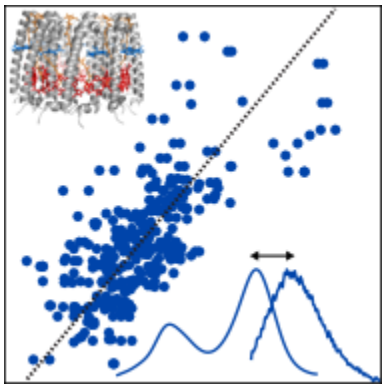

KEYWORDS Single Molecule, Fourier-transform spectroscopy, spectral variability, disorder, Stokes shift, light harvesting complex LH2.

Over billions of years, Nature has developed and optimized an efficient and sustainable method to produce energy: photosynthesis. The process begins with the capturing of light energy by light-harvesting antenna complexes, which is then dissipated via excitonic transfer to a reaction center where the photochemical energy conversion takes place. The antenna complexes are quite robust to environmental changes; they are able to handle several magnitudes of light intensity[1,2], they adapt to spectral changes[1] and the photon energy transfer has 80-95% efficiency under ideal conditions[3,4].

As the main actors in the capturing of energy to fuel life on Earth, light-harvesting complexes have been investigated by a wide range of spectroscopies[5–9]. Especially in the last decade, two-dimensional electron spectroscopy (2D-ES) has revealed intrinsic details on the internal coupling and energy transfer paths of the multi-chromophoric antenna complexes[5,10,11] including persistent coherent responses which have been observed even under physiological conditions[5,12–14]. In ensemble measurements, the collective oscillatory response over many complexes is measured. The spectral and dynamical disorder due to variations in the dipolar interactions between the chromophores of different complexes often makes it too complex to interpret in detail. At the single complex level, the individual oscillatory traces are resolved at the cost of weak signals[13].

Due to its highly symmetric structure[15,16], the light harvesting complex LH2, a pigment-protein complex of the purple bacteria *Rps. Acidophila,* has been studied extensively at both cryogenic[17–22] and ambient[2,23,24] temperatures. It contains 27 bacteriochlorophyll (*BChl a*) pigments that are arranged into two concentric rings called B800 and B850 according to their absorption maxima. The nine well-separated pigments of the B800 ring act localized and the 18 tightly packed pigments of the B850 ring form a delocalized excitonic state. Emission occurs from the B850 band, with a fluorescence quantum yield of about 10%. The spectra of single LH2 complexes were first resolved at cryogenic temperature, revealing individual chromophore bands, coupling in broadened excitonic bands, heterogeneity, energy disorder, spectral diffusion, and polarization response[25]. Under physiological conditions, the inherent low fluorescence quantum yield, and limited photostability has so far constrained single complex studies to the recording of emission spectra, where spectral inhomogeneities including intrinsic and environmentally induced spectral variability and photoinduced spectral diffusion, jumps, and blinking manifest themselves[2].

Recently, we have addressed the excited state energy transfer dynamics of single LH2 complexes under ambient conditions by fs pump-probe excitation, revealing transient fs traces that exhibit long-lived quantum coherences with oscillation periods between 140 and 400 fs[13]. This large spread is related to the distribution in energy disorder between complexes, which is an important parameter in the modeling and interpretation of the behavior of LH2[26]. While some tentative conclusions about the excited state behavior can be drawn from single complex emission spectra[17,24,27,28], the actual spectra of the excited state manifold, where these coherences take place, are still lacking. Therefore, it would be a great asset both to experiments and to modeling to acquire single complex excitation and emission spectra available side by side.

In this Letter, we quantify the inhomogeneity of the excitation and emission bands and their mutual correlations. We focus on the variation in spectral band positions and interband distances with a special interest in the Stokes shift. To measure the excitation spectra, we adapted our robust Fourier transform excitation spectroscopy[29] to operate at the low light conditions required to avoid photoactivated effects and stably record individual LH2 complexes. Due to its ability to measure weakly fluorescing, instable particles, the approach can be applied to a broad range of systems.

We measured excitation and emission spectra of hundreds of individual LH2 complexes with the 750 – 880 nm wavelength range of a broadband laser (Octavius-85M, Thorlabs). Either the spectrally separated B800 and emission bands were measured simultaneously, or the spectrally overlapping full excitation and emission spectra were measured sequentially. When measuring sequentially, the switching between the two microscope ports and excitation bandwidths occurred manually and took a few seconds. To ensure the signal stability in this case, first an excitation spectrum was measured, then an emission spectrum, and finally another excitation spectrum. In case of significant differences between the two excitation spectra the results were discarded. All measurements were performed at low excitation powers around 100W/cm^2 to avoid photoactivated spectral instabilities[23] and saturation effects[30], both of which already emerge at moderate excitation powers. Going to higher powers would significantly reduce the photostability without gaining much signal strength due to saturation. The results of the simultaneous and sequential measured are presented without distinction when not explicitly stated otherwise.

For the excitation spectra, interferograms were recorded with a delay line, which was continuously scanned over approximately 400 fs (600 μm) with a speed of 1 nm/s, resulting in 1 scan per minute. Around 10-30 fluorescence counts were obtained for time bins of 20ms after subtraction of the interferogram of the laser light leaking through the filters (around 2 counts/20ms). **Figure 1**a shows an example of four consecutive scans using the full spectral width on a somewhat unstable LH2 complex exhibiting some blinking. The low fluorescence quantum yield together with the low excitation power resulted in a poor signal-to-noise ratio, which needed to be countered by careful data processing. **Figure 1**b demonstrates the effect of the data processing on the scans. A single scan (red) has a noticeably lower signal-to-noise ratio than the four averaged scans, for which all blinking events are excluded from the averaging (green). Consequentially, the applied Hann-window suppresses the signal far from time zero, which mainly consists of noise (blue). **Figure 1**c shows the corresponding excitation spectra which were obtained by a Fourier transformation followed by a division by the laser spectrum added in gray to the last graph[29]. The two absorption bands become visible only after averaging and removal of the blinking events while the spectra become much smoother after windowing. Increasing the sampling frequency through zero-padding (black dashed lines) resolves the peaks better without changing the results otherwise. Emission spectra were recorded as an accumulation of 1 s measurements. A series of up to 4 minutes was accumulated and the background signal removed.

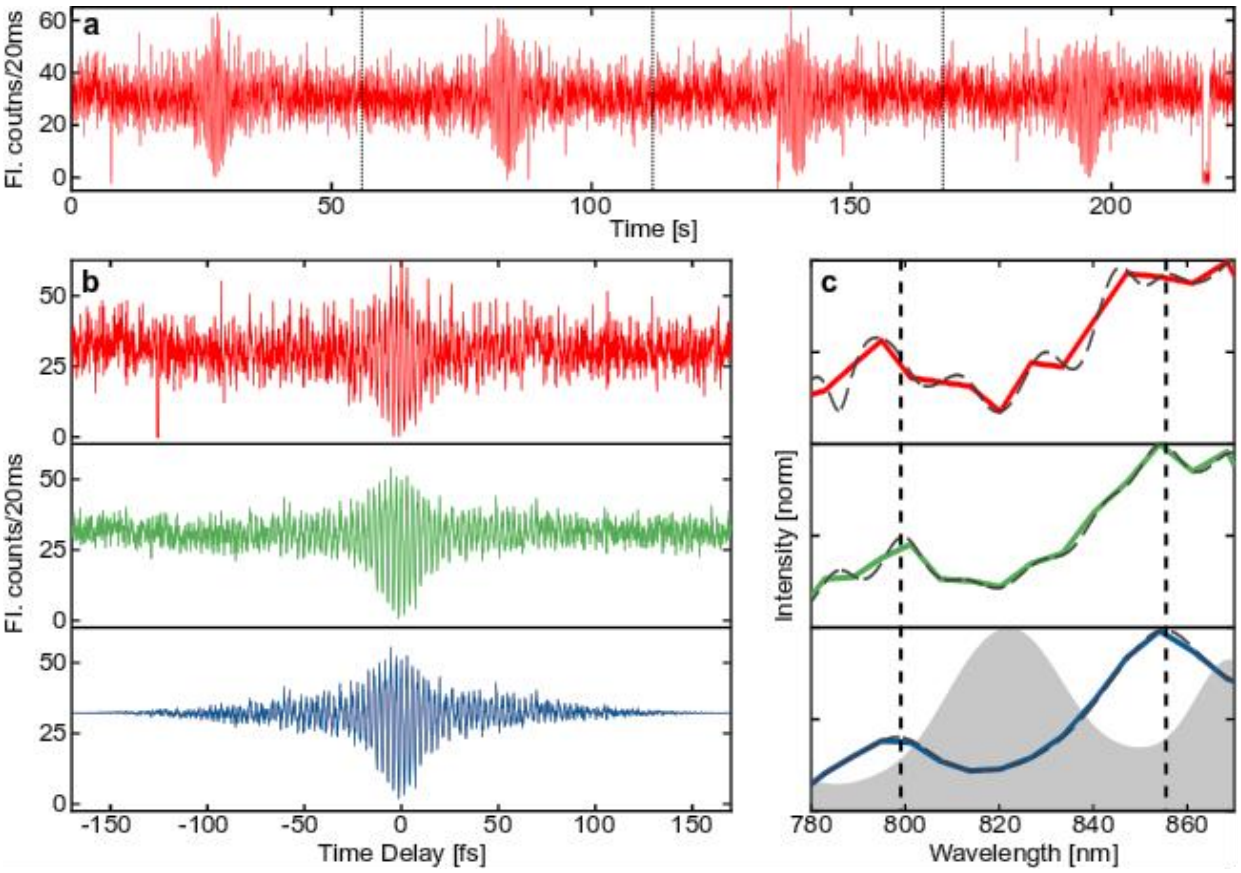

Figure 1 Single molecule Fourier-transform excitation spectroscopy. (a) Four consecutive time delay scans of the same single LH2 complex. (b) The first scan (red), the 4 corrected scans averaged (green) also with windowing added (blue). (c) Resulting excitation spectrum after Fourier transformation of the interferograms of (b) and division by the laser spectrum. The dashed black lines have zero-padding added to increase the sampling frequency and the vertical lines are added as a guide to the eye. The laser excitation spectrum is shown in gray.

Figure 2a shows the spectrum obtained when summing the not-normalized spectra of hundreds of individual complexes (solid lines). The same graph also shows the average over ensemble spectra measured on 12 different positions of a thin film sample (dashed lines). For the thin film and the single complex studies, the same sample preparation and measurement protocols were used and only the concentration of LH2 complexes changed. The sum spectrum resembles the thin film spectrum well despite the spectral heterogeneity of the individual spectra even though LH2 complexes were mainly surrounded by other LH2 complexes in the thin film sample, and by the polymer matrix in the single LH2 sample. This demonstrates the effectiveness of the protein scaffold of the LH2 complexes at protecting the pigments from their environment. **Figure 2b-f** shows representative examples of excitation and emission spectra measured sequentially on individual LH2 complexes where the B850 band varies between approximately 840 nm and 870 nm, while the emission spectrum remains at a relatively constant position. The subtle differences between the individual spectra will be studied statistically in the following.

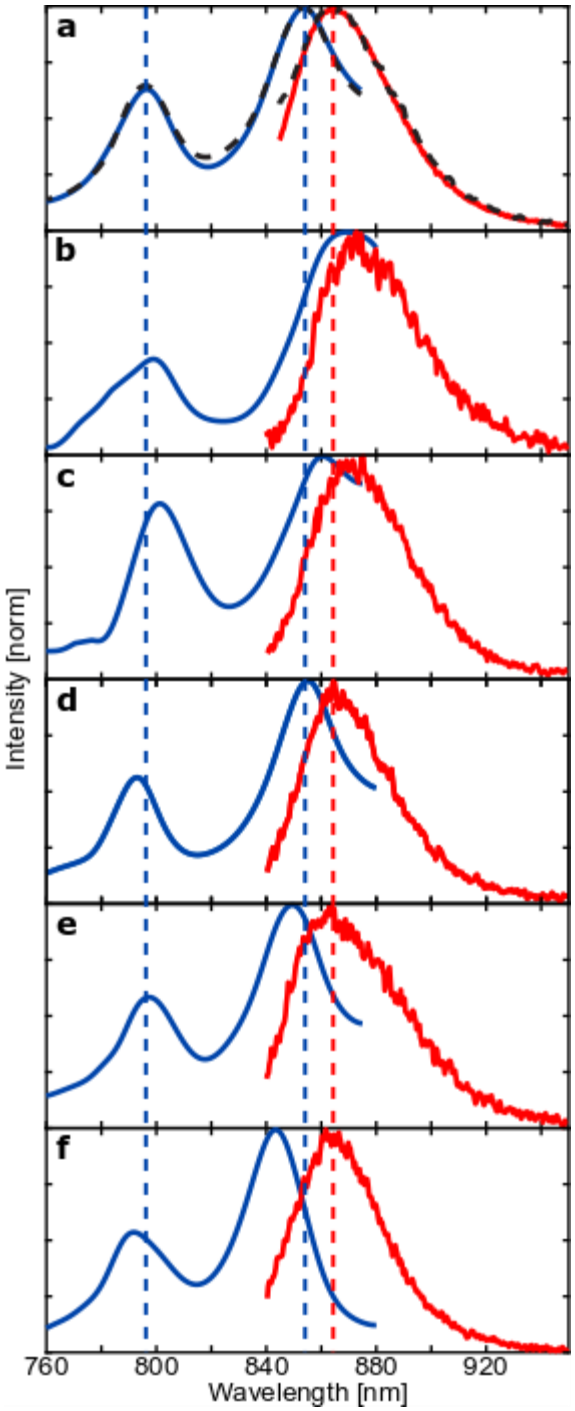

Figure 2: Single LH2 room temperature excitation and emission spectra. (a) The sum of all measured excitation (blue) and emission (red) spectra alongside the thin film spectra (black dashed line). (b-f) Excitation (blue) and emission (red) spectra of five distinct LH2 complexes showing differences in B850 band position while having comparable emission spectra. Dashed lines: thin film results.

	B800	B850	Emission
Sum spectrum	796.5 nm	853.8 nm	864.7 nm
Thin film spectrum	796.1 (0.2) nm	853.8 (0.5) nm	864.8 (1.1) nm
Single complex	796.1 (3.6) nm	853.7 (5.4) nm	866.0 (5.4) nm

Table 1 Peak positions. The band positions for the sum of all single complex spectra, and the average (and standard deviation) for individual thin film, and single complex measurements.

To quantify the results, the peak positions of the sum, thin film and single complex spectra were determined using the peak finder function of Matlab for the excitation spectra and a skewed Gaussian fit[2] for the emission spectra. Table 1 gives the average values of the band positions (and their standard deviation). The three values agree well with one other even though the B800 and emission band are blue-shifted by approximately 3 nm and the B850 band by 5 nm compared to thin film ensemble results published elsewhere[6]. Small offsets in the spectral calibration cannot be completely ruled out but since the B800 and B850 band were measured together, their interband distance should be conserved. We therefore assign this discrepancy to differences in the sample preparation conditions and environments[6,17,31].

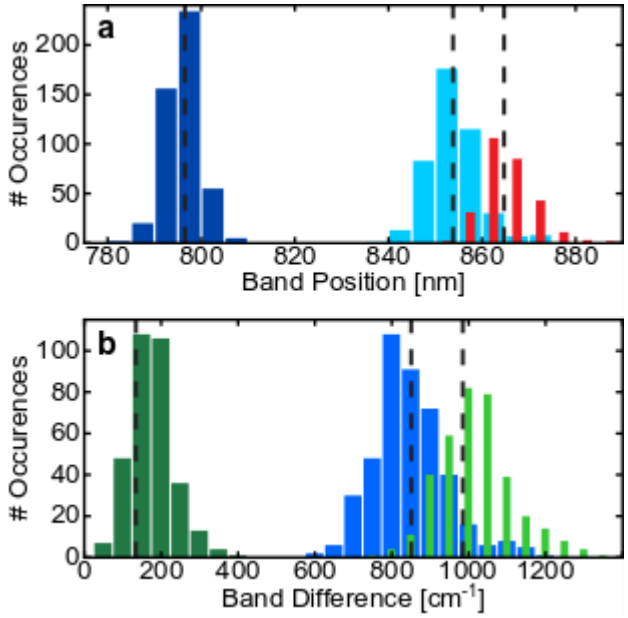

Figure 3: Distribution of peak positions and interband distances. (a) The distribution of the position of the B800 (dark blue), B850 (light blue) and emission (red) band. (b) The interband distance between B850 – emission, i.e. Stokes shift (dark green), B800-B850 (blue) and B800-emission (light green).

Figure 3a depicts the distribution of the peak positions of the excitation and emission bands for a better visualization of the spectral variability. The dashed lines indicate the average values of the thin film measurements for comparison. The distribution of the B800 band (dark blue, FWHM 133 cm^{-1}) is narrower than that of the B850 band (light blue, FWHM 173 cm^{-1}) or the emission band (red, FWHM 168 cm^{-1}), which have a similar width. This is because the chromophores of the B800 ring are weakly coupled, which makes them less sensitive to environmental changes than the strongly coupled B850 ring, and which leads to a narrower B800 distribution. Emission takes place from the B850 band, which is reflected in the similar widths of the two distributions. Previous measurements on emission spectra already reported that the distribution of peak position broadens significantly for higher excitation powers[23]. The narrowness of the distribution observed here confirms that we are in a weak excitation regime where we avoided photoinduced effects to best resemble physiological conditions.

	B800 – B850	**B800 – Emission**	**Stokes shift**
Sum spectrum	843 cm^{-1}	978 cm^{-1}	136 cm^{-1}
Thin film spectrum	848 (8) cm^{-1}	991 (6) cm^{-1}	144 (9) cm^{-1}
Single complex	845 (96) cm^{-1}	1019 (96) cm^{-1}	177 (58) cm^{-1}

Table 2: Interband distances. The interband distances between the two absorption and the emission band the sum of all single complex spectra, and the average (and standard deviation) for individual thin film, and single complex measurements.

As was already apparent from **Figure 2**, the interband distances are not constant, but vary from complex to complex. **Table 2** summarizes these distances, and the sum, thin film and single complex spectra are in agreement. **Figure 3**b shows the distribution of the interband distances between the B850 and the emission band, i.e. the Stokes shift (dark green, FWHM 135 cm^{-1}), the B800 and B850 band (blue, FWHM 226 cm^{-1}) as well as the B800 and emission band (light green, FWHM 225 cm^{-1}). Dashed lines again indicate the corresponding thin film values. Even though the spectral position of the B850 and emission band have a wider distribution than the B800 band, their interband distance is the least variable. This pinpoints towards a correlation between the B850 and emission band position.

To verify this correlation, we relate the individual peak positions in scatter plots in Figure 4 with the complexes presented in **Figure 2** highlighted in red. The B800 band position is indeed uncorrelated with either the B850 or emission band (**Figure 4**a resp. b) while the B850 and emission band positions exhibit a linear correlation (**Figure 4**c). This reinforces the observation that the B800 and B850 bands react independently to their nanoenvironment due to different coupling strengths between their pigments. Emission takes place from the B850 band, so that these two bands are correlated.

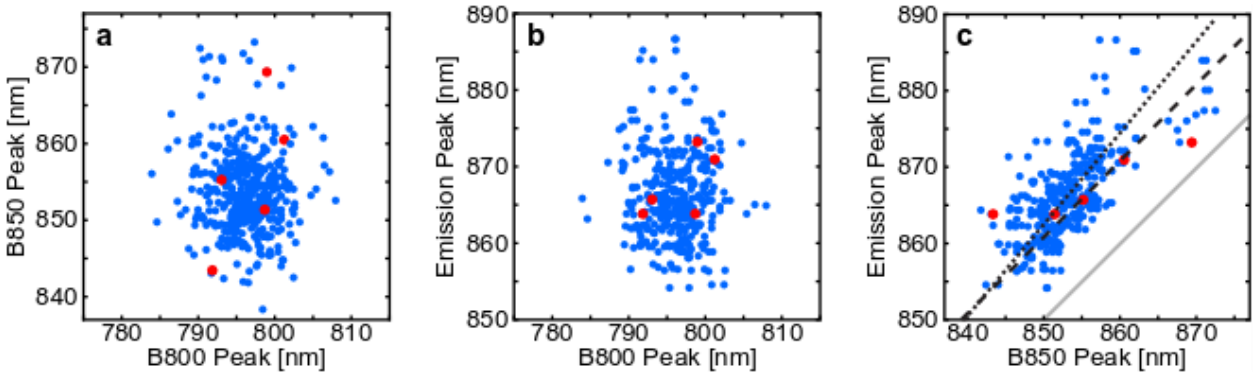

Figure 4: Scatter plots of band positions. (a) B800 vs B850 band, (b) B800 vs emission band and (c) B850 vs emission band. The dashed line indicates the interpolated value of the thin film result assuming a constant Stokes shift and the dotted line the total least square fit. The solid gray line is the unit-line. The red dots correspond to the spectra in Figure 2.

Still, the correlation in **Figure 4**c exhibits a wide distribution of points over a relatively narrow spectral range, making it difficult to determine the linear dependency of the Stokes shift on the band position. Interpolating the thin film results under the assumption of a constant Stokes shift, i.e. a line with slope 1, appears to be a good first approximation (dashed line). With a total least square fit, a slope of 1.2 is obtained, resulting in a larger Stokes shift for more red-shifted complexes (dotted line). This reinforces the model presented by Novoderezhkin et al. which predicted this behavior as a consequence of static disorder and differences in couplings to phonons[27]. In their model, spectra shifted to higher wavelengths featured excitonic energy levels that were more split, leading to fluorescence emission mainly occurring from more red-shifted energy levels. Still the spread in Stokes shift is much larger than the maximum inaccuracy for the interband distances of about 30 cm^{-1}, estimated from repeated measurements on the same weakly fluorescing complexes, so that the slope only represents a general trend.

The dashed line in **Figure 4**c is located towards the bottom of the data points of the scatter plot because the mean position of the sum and thin film results which are blue-shifted by about 1.5 nm with respect to the single complex emission spectra (see **Table 1**). This difference can be explained by an on average larger peak intensity for blue-shifted complexes, whose positions are then weighted more in the case of sum and thin film spectra, but not for the single complex case. The excitation spectra did not exhibit the same intensity bias because their intensity scales with the total rather than the peak fluorescence intensity. For brighter, blue-shifted complexes, a larger fraction of the total fluorescence intensity is blocked by the laser cleanup filter, resulting in comparable intensities for all spectral positions. The one-sided intensity bias consequentially resulted in a difference of around 35 cm^{-1} between the Stokes shift measured on individual complexes and the ensemble (see **Table 2**). This illustrates how going to the single particle level does not only lift the ensemble average, but also removes biases imposed by the experimental parameters.

Overall, we have demonstrated that it is feasible to record excitation and emission spectra of individual LH2 complexes under physiological conditions. For this, we have matured our broadband Fourier transform excitation spectroscopy method from proof-of-principle experiments on synthetic dyes to measurements on biologically relevant systems, demonstrating its potential as a spectroscopic tool to access to the excited state manifold. The instability inherent to LH2 complexes at room temperature was circumvented by going to low excitation powers while the resulting low signal levels were overcome by effective data analysis. The results show a remarkably little spectral variation (130-170 cm^{-1}), far below that observed for isolated dye molecules. The lack of correlation between the B800 and B850 band manifests that the two rings react to environmental changes independently, one being weakly and the other strongly coupled. The single complex Stokes shift showed variations and the shift is on average larger for red-shifted complexes and about 20% larger than the ensemble Stokes shift. With the quantification of this disorder, we provided important variables for both models and the interpretation of experimental results, which will not least help with the interpretation of the observed long-lasting coherences. This method can be applied to a wide range of systems including those that are weakly fluorescing or with low photostability.

Experimental Methods

Sample preparation. LH2 was purified from Rps. acidophila (strain 10050)[32], diluted in aqueous PVA solution (10mM Na2HPO4 pH 8.1, 0.03% α-dodecyl maltoside) and spin-coated on a #1 glass coverslip at 1500 rpm for 60 s. For single molecule studies the dilution was 80000x and for the thin film 12x. Oxygen was removed from the sample by a constant nitrogen flow.

Excitation-emission setup. The experimental setup was adapted from [29]. The 750 – 880 nm wavelength range of a broadband laser was selected and propagated through the interferometer (NRT 100/M, Thorlabs or M-230.10, Physik Instrumente). In the microscope, the interfering pulse pairs were reflected from a 10/90 beamsplitter and focused to a diffraction-limited spot on the sample (1.4NA, 60x, Nikon Plan Apo λ). The fluorescence was collected in reflection and sent to the EMCCD camera for emission spectroscopy or to the APD for confocal optical imaging and excitation spectroscopy. Excitation took place with about 6 μW light intensity measured at the microscope entrance (~100W/cm^2 at sample). For the simultaneous measurements, the laser above 820 nm was blocked (tilted 842SP, Semrock) and the laser light was blocked in the detection path (2x830LP, Semrock). Using a 50/50 beamsplitter, the fluorescence signal was then sent to an electron-multiplying charge-coupled device (EMCCD) camera (Newton 971, Andor) for the emission spectra and an avalanche photo diode (APD, Perkin-Elmer) for the excitation spectra. For sequential measurement, emission spectra were measured the same way as for the simultaneous measurements. Excitation spectra were recorded with the full laser bandwidth and detected by the APD at a separate microscope output port (2x885LP, AHF).

Acknowledgements

The authors thank Lisa Saemisch, Richard Lane, and Vikas Remesh for help with sample preparation, and Matz Liebel and Lukasz Piatkowski for useful spectroscopic discussions. E.G. acknowledges financial support by the Ministry of Economy ("Severo Ochoa" SEV-2014-0124). N.F.v.H. acknowledges the financial support by the European Commission (ERC Advanced Grant 670949-LightNet), Ministry of Science, Innovation and Universities (MCIU/AEI: PGC2018-096875-B-I00), Ministry of Economy (MINECO: "Severo Ochoa" program for Centers of Excellence in R&D SEV-2015-0522 and Plan Nacional FIS2015-69258-P), the Catalan AGAUR (2017SGR1369), Fundació Privada Cellex, Fundació Privada Mir-Puig, and Generalitat de Catalunya through the CERCA program. Finally, R.C. thanks the Biotechnology and Biological Sciences Research Council (BBSRC) for financial support.

References

(1) Croce, R.; Amerongen, H. van. Natural strategies for photosynthetic light harvesting. *Nat. Chem. Biol.* **2014**, *10*, 492–501, DOI: 10.1038/nchembio.1555.

(2) Rutkauskas, D.; Novoderezkhin, V.; Cogdell, R. J.; Grondelle, R. van. Fluorescence Spectral Fluctuations of Single LH2 Complexes from Rhodopseudomonas acidophila Strain 10050. *Biochemistry (Mosc.)* **2004**, *43*, 4431–4438, DOI: 10.1021/bi0497648.

(3) Blankenship, R. E.; Tiede, D. M.; Barber, J.; Brudvig, G. W.; Fleming, G.; Ghirardi, M.; Gunner, M. R.; Junge, W.; Kramer, D. M.; Melis, A.; Moore, T. A.; Moser, C. C.; Nocera, D. G.; Nozik, A. J.; Ort, D. R.; Parson, W. W.; Prince, R. C.; Sayre, R. T. Comparing Photosynthetic and Photovoltaic Efficiencies and Recognizing the Potential for Improvement. *Science* **2011**, *332*, 805–809, DOI: 10.1126/science.1200165.

(4) Blankenship, R. E. Molecular Mechanisms of Photosynthesis. **2014**.

(5) Harel, E.; Engel, G. S. Quantum coherence spectroscopy reveals complex dynamics in bacterial light-harvesting complex 2 (LH2). *Proc. Natl. Acad. Sci. U.S.A.* **2012**, *109*, 706–711, DOI: 10.1073/pnas.1110312109.

(6) Kunz, R.; Timpmann, K.; Southall, J.; Cogdell, J. RichTimpmann Köhler; Freiberg, A. Fluorescence-Excitation and Emission Spectra from LH2 Antenna Complexes of Rhodopseudomonas acidophila as a Function of the Sample Preparation Conditions. *J. Phys. Chem. B* **2013**, *117*, 12020–12029, DOI: 10.1021/jp4073697.

(7) Gottfried, D. S.; Stocker, J. W.; Boxer, S. G. Stark effect spectroscopy of bacteriochlorophyll in light-harvesting complexes from photosynthetic bacteria. *Biochim. Biophys. Acta, Bioenerg.* **1991**, *1059*, 63–75, DOI: 10.1016/s0005-2728(05)80188-4.

(8) Visschers, R. W.; Germeroth, L.; Michel, H.; Monshouwer, R.; Grondelle, R. van. Spectroscopic properties of the light-harvesting complexes from Rhodospirillum molischianum. *Biochim. Biophys. Acta, Bioenerg.* **1995**, *1230*, 147–154, DOI: 10.1016/0005-2728(95)00046-l.

(9) Fleming, G. R.; Grondelle, R. van. Femtosecond spectroscopy of photosynthetic light-harvesting systems. *Curr. Opin. Struct. Biol.* **1997**, *7*, 738–748, DOI: 10.1016/s0959-440x(97)80086-3.

(10) Engel, G. S.; Calhoun, T. R.; Read, E. L.; Ahn, T.-K.; Mancal, T.; Cheng, Y.-C.; Blankenship, R. E.; Fleming, G. R. Evidence for wavelike energy transfer through quantum coherence in photosynthetic systems. *Nature* **2007**, *446*, 782, DOI: 10.1038/nature05678.

(11) Thyrhaug, E.; Tempelaar, R.; Alcocer, M. J. P.; Zidek, K.; Bina, D.; Knoester, J.; Jansen, T. L. C.; Zigmantas, D. Identification and characterization of diverse coherences in the Fenna-Matthews-Olson complex. *Nat. Chem.* **2018**, *10*, 780–786, DOI: 10.1038/s41557-018-0060-5.

(12) Cheng, Y. C.; Silbey, R. J. Coherence in the B800 Ring of Purple Bacteria LH2. *Phys. Rev. Lett.* **2006**, *96*, 028103–, DOI: 10.1103/PhysRevLett.96.028103.

(13) Hildner, R.; Brinks, D.; Nieder, J. B.; Cogdell, R. J.; Hulst, N. F. van. Quantum Coherent Energy Transfer over Varying Pathways in Single Light-Harvesting Complexes. *Science* **2013**, *340*, 1448–1451, DOI: 10.1126/science.1235820.

(14) Sumi, H. Bacterial photosynthesis begins with quantum-mechanical coherence. *Chem. Rec.* **2001**, *1*, 480–493, DOI: 10.1002/tcr.10004.

(15) McDermott, G.; Prince, S. M.; Freer, A. A.; Hawthornthwaite-Lawless, A. M.; Papiz, M. Z.; Cogdell, R. J.; Isaacs, N. W. Crystal structure of an integral membrane light-harvesting complex from. *Nature* **1995**, *374*, 517–521, DOI: 10.1038/374517a0.

(16) Papiz, M. Z.; Prince, S. M.; Howard, T.; Cogdell, R. J.; Isaacs, N. W. The Structure and Thermal Motion of the B800-850 LH2 Complex from Rps. acidophila at 2.0 Å Resolution and 100 K: New Structural Features and Functionally Relevant Motions. *J. Mol. Biol.* **2003**, *326*, 1523–1538, DOI: 10.1016/s0022-2836(03)00024-x.

(17) Bopp, M. A.; Sytnik, A.; Howard, T. D.; Cogdell, R. J.; Hochstrasser, R. M. The dynamics of structural deformations of immobilized single light-harvesting complexes. *Proc. Natl. Acad. Sci. U.S.A.* **1999**, *96*, 11271–11276, DOI: 10.1073/pnas.96.20.11271.

(18) Hofmann, C.; Aartsma, T. J.; Michel, H.; J., K. Direct observation of tiers in the energy landscape of a chromoprotein: A single-molecule study. *Proc. Natl. Acad. Sci. U.S.A.* **2003**, *100*, 15534–15538, DOI: 10.1073/pnas.2533896100.

(19) Kunz, R.; Timpmann, K.; Southall, J.; Cogdell, R. J.; Freiberg, A.; Köhler, J. Single-Molecule Spectroscopy Unmasks the Lowest Exciton State of the B850 Assembly in LH2 from Rps. acidophila. *Biophys. J.* **2014**, *106*, 2008–2016, DOI: 10.1016/j.bpj.2014.03.023.

(20) Matsushita, M.; Ketelaars, M.; Oijen, A. M. van; J., K.; Aartsma, T. J.; Schmidt, J. Spectroscopy on the B850 Band of Individual Light-Harvesting 2 Complexes of Rhodopseudomonas acidophila II. Exciton States of an

Elliptically Deformed Ring Aggregate. *Biophys. J.* **2001**, *80*, 1604–1614, DOI: 10.1016/S0006-3495(01)76133-4.
(21) Oijen, A. M. van; Ketelaars, M.; Köhler, J.; Aartsma, T. J.; Schmidt, J. Unraveling the Electronic Structure of Individual Photosynthetic Pigment-Protein Complexes. *Science* **1999**, *285*, 400–402, DOI: 10.1126/science.285.5426.400.
(22) Zerlauskiene, O.; Trinkunas, G.; Gall, A.; Robert, B.; Urboniene, V.; Valkunas, L. Static and Dynamic Protein Impact on Electronic Properties of Light-Harvesting Complex LH2. *J. Phys. Chem. B* **2008**, *112*, 15883–15892, DOI: 10.1021/jp803439w.
(23) Rutkauskas, D.; Novoderezhkin, V.; Cogdell, R. J.; Grondelle, R. van. RETRACTED: Fluorescence Spectroscopy of Conformational Changes of Single LH2 Complexes. *Biophys. J.* **2005**, *88*, 422–435, DOI: 10.1529/biophysj.104.048629.
(24) Schlau-Cohen, G. S.; Wang, Q.; Southall, J.; Cogdell, R. J.; Moerner, W. E. Single-molecule spectroscopy reveals photosynthetic LH2 complexes switch between emissive states. *Proc. Natl. Acad. Sci. U.S.A.* **2013**, *110*, 10899–10903, DOI: 10.1073/pnas.1310222110.
(25) Oijen, A. M. van; Ketelaars, M.; Köhler, J.; Aartsma, T. J.; Schmidt, J. Spectroscopy of Single Light-Harvesting Complexes from Purple Photosynthetic Bacteria at 1.2 K. *J. Phys. Chem. B* **1998**, *102*, 9363–9366, DOI: 10.1021/jp9830629.
(26) Caycedo-Soler, F.; Lim, J.; Oviedo-Casado, S.; Hulst, N. F. van; Huelga, S. F.; Plenio, M. B. Theory of Excitonic Delocalization for Robust Vibronic Dynamics in LH2. *J. Phys. Chem. Lett.* **2018**, *9*, 3446–3453, DOI: 10.1021/acs.jpclett.8b00933.
(27) Novoderezhkin, V. I.; Rutkauskas, D.; Grondelle, R. van. Dynamics of the Emission Spectrum of a Single LH2 Complex: Interplay of Slow and Fast Nuclear Motions. *Biophys. J.* **2006**, *90*, 2890–2902, DOI: 10.1529/biophysj.105.072652.
(28) Tubasum, S.; Camacho, R.; Meyer, M.; Yadav, D.; Cogdell, R. J.; Pullerits, T.; Scheblykin, I. G. Evidence of excited state localization and static disorder in LH2 investigated by 2D-polarization single-molecule imaging at room temperature. *Phys. Chem. Chem. Phys.* **2013**, *15*, 19862–19869, DOI: 10.1039/C3CP52127C.
(29) Piatkowski, L.; Gellings, E.; Hulst, N. F. van. Broadband single-molecule excitation spectroscopy. *Nat. Commun.* **2016**, *7*, 10411, DOI: 10.1038/ncomms10411.
(30) Wientjes, E.; Renger, J.; Cogdell, R.; Hulst, N. F. van. Pushing the Photon Limit: Nanoantennas Increase Maximal Photon Stream and Total Photon Number. *J. Phys. Chem. Lett.* **2016**, *7*, 1604–1609, DOI: 10.1021/acs.jpclett.6b00491.
(31) Richter, M. F.; Baier, J.; Cogdell, R. J.; Köhler, J.; Oellerich, S. Single-Molecule Spectroscopic Characterization of Light-Harvesting 2 Complexes Reconstituted into Model Membranes. *Biophysical Journal* **2007**, *93*, 183–191, DOI: 10.1529/biophysj.106.103606.
(32) Gardiner, A. T.; Takaichi, S.; Cogdell, R. J. The effect of changes in light intensity and temperature on the peripheral antenna of Rhodopseudomonas acidophila. *Biochem. Soc. Trans.* **1993**, *21*, 6S–6S, DOI: 10.1042/bst021006s.